Bistability of optical guided-wave beam deflector

LI Yushan, LIN Shengqiang, and JIN Feng
Changchun Institute of Physics, Academia Sinica

WANG Yongxing
The First Optical Instrument Factory of Changchun

(Received 17 December 1982; revised 16 February 1983)
Acta Opt. Sin. **3**(8), 685–690 (November 1983)

The bistability of the beam deflector has been demonstrated using an $LiNbO_3$ waveguide electro-optic prism. For this, using the Gaussian function model of the modulation characteristic curve, the necessary theoretical analysis has been carried out and agrees basically with the measured results.

PACS numbers: 42.80.Ks, 42.80.Em, 42.80.Lt, 42.82. + n

I. INTRODUCTION

In the field of integrated optics, the phase modulation was converted into the intensity modulation for the electro-optic waveguide modulator using the interference, directional coupling, cutoff, and other effects. Many hybrid optical bistability devices were achieved by the electrical feedback, such as the phase modulator with a Fabry-Perot cavity,[1,2] the amplitude modulator of the multimode waveguide without cavity,[3] the directional coupling modulator,[4,5] the two arm interference modulator,[6,7] and cutoff modulator.[8,9] Except these optical waveguide modulators, the guided-wave beam deflector also can be used in principle to construct the optical bistable device. In this paper, the optical bistability of the beam deflector has been demonstrated using an $LiNbO_3$ waveguide electro-optic prism.[10,11] The Gaussian function model of the modulation characteristic curve was presented and the necessary theoretical analysis was carried out.

II. THE EXPERIMENTAL SETUP

The experimental setup is shown in Fig. 1. Here, an $LiNbO_3$ waveguide electro-optic prism[1] was used as the beam deflector. It is formed of parallel electrodes and an oblique electrode 9 along the X axis on the Y-cut Ti-diffused $LiNbO_3$ crystal using photolithography technology. The gap between the parallel electrodes was divided into two electro-optic prism regions by the oblique electrode. The opposite-pole electrical fields along the Z axis were applied in the two regions, a refractive index difference is produced by the linear electro-optic effect, and then the TE wave was deflected in the waveguide plane through the electrodes. When this device was served as bipolar switch, its switching voltage and time are $\pm$ 19 V and 0.1 ns, respectively, for the He-Ne laser ($\lambda = 6328$ Å) and 50 Ω load.

The input prism 2 and output prism 3 were the input and output couplers of the waveguide, respectively, and were used to couple the He-Ne laser of TE polarization into and out of the waveguide. The input detector 5 was used to detect the intensity of input light through the beam splitter 4.

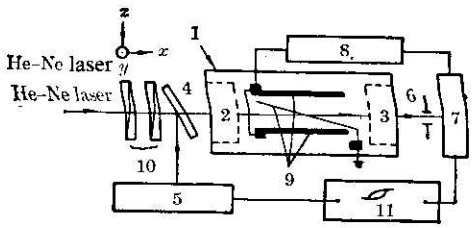

FIG. 1. Schematic diagram of the experimental setup.

 0273-429X/84/020418-06$06.50

The output detector 7 was used to detect the deflected output light beam by one-dimensional sampling through the sampling slit 6. The current signal of the output detector was amplified into a voltage signal by an electrical amplifier, and was applied on the electrodes of the electro-optic prism so that the electrical feedback was achieved. The bias voltage of the device was provided directly by the amplifier, so the bias circuit was omitted. The optical attenuator 10 consists of two polarizers, and was used to change the input light intensity.

When the input and output detectors were connected with the recorder 11 and the input light intensity was changed continuously by using the optical attenuator 10, the input-output characteristic curves of the device are plotted by the recorder. The shapes of these characteristic curves are dependent on the voltage, the position and width of the sampling slit, and the intensity of the background light, and the bistable hysteresis curves were formed under certain conditions.

III. THEORETICAL ANALYSIS

The two-dimensional Gaussian light beam was coupled into the optical waveguide by the input prism and was changed into one-dimensional Gaussian light beam in the waveguide plane. It was deflected through the electrodes. The light beam coupled from output prism has the approximate Gaussian intensity profile along the direction parallel to the waveguide plane. When the direction of the sampling slit is perpendicular to guide plane and the slit width is smaller than the output beam aperture, then for any given input light intensity and slit position, the relation between the sampling output light intensity I and the modulation voltage V (the modulation characteristics of the device) can be expressed approximately by Gaussian functions:

$$I/I_m = D = \exp[-(V-V_m)^2/V_d^2], \tag{1}$$

where I_m is the maximum value of I (corresponding to the situation that the center part of the Gaussian beam enters into the sampling slit), and is proportional to the input light intensity. D is the normalized detection coefficient. V_m is the modulation voltage when $I = I_m$, and is dependent on the position of the sampling slit. V_d is used to represent the width of the D-V curve, and is dependent on the bipolar switching voltage and the slit width of the device. For convenience, we have used I_m to represent the input light intensity and the I-I_m relation to describe the input-output characteristics of the device in this paper.

The optical guided-wave beam is scattered in the waveguide plane because of the irregularities of the guide surface and the refractive index, thus m lines are broadened. Therefore, the m line together with the scattered light constitutes the background light. Assuming that D_s is the contribution of the background light to D, then Eq. (1) can be rewritten as

$$D = D_s + (1-D_s)\exp[-(V-V_m)^2/V_d^2] \ , \tag{2}$$

when the deflected angle of the beam is very small; D_s is approximately constant. It is seen from this that the background light influences the modulation character of the device, especially the m line.

For the linear feedback, the modulation voltage can be expressed as $V = V_B + K_I I$, where V_B is bias voltage, and K_I is the feedback coefficient of I to V. Thus, the feedback character of the device can be expressed as

$$I/I_m = D = (V-V_B)/K_I I_m \ . \tag{3}$$

The modulation characteristic curve of Gaussian model (denoted as the modulation curve) was plotted by Eq. (2), and two feedback characteristic curves tangent to the modulation curve (denoted as the feedback curve) were plotted by Eq. (3), for the given bias voltage V_B. These curves are shown in Fig. 2. Within the region between these two feedback curves, an arbitrary feedback curve always has three intersections with the modulation curve. The middle intersec-

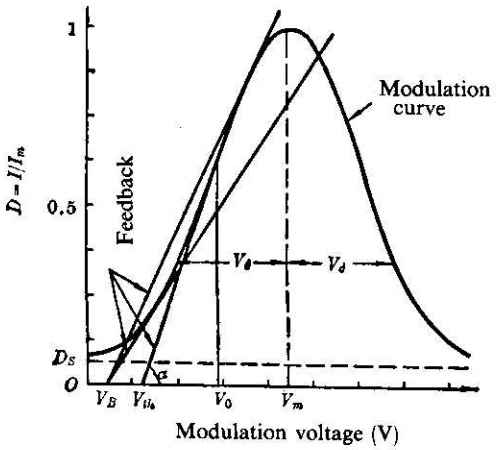

FIG. 2. The Gaussian modulation characteristic curve.

tion corresponds to an unstable state. The other two intersections correspond to bistable state; that is, there exist two stable output states for a given input state. Within the regions outside these two feedback curves, an arbitrary feedback curve has only one intersection with the modulation curve, hence there is only one stable output state for a given input state.

If two feedback curves tangent to the modulation curve overlap with each other and are also tangent to the inflection point of the modulation curve, then the device is operating at the critical state, that is, the transition from the bistable state to single stable state. In Fig. 2, the feedback curve tangent to the inflection point of the modulation curve was plotted, and the angle between this tangent line and abscissa axis is defined as α. Thus the threshold bias voltage of achieving the bistability can be expressed as

$$V_{th}=V_0-D(V_0)/\mathrm{tg}\,\alpha=V_0-D(V_0)/(dD/dV)_{V=V_0}, \tag{4}$$

where V_0 is the modulation voltage corresponding to the inflection point. For the modulation curve of the Gaussian model, we can derive from Eq. (2) and Eq. (4) that

$$V_0=V_m-(V_d/\sqrt{2}), \tag{5}$$

$$V_{th}=V_m-\sqrt{2}\,V_d\left[1+\frac{D_s\sqrt{e}}{2(1-D_s)}\right]. \tag{6}$$

Obviously, V_{th} is dependent on V_m, V_d, and D_s. In other words, the threshold bias voltage is dependent on the width and position of the sampling slit, the bipolar switching voltage, and the intensity of the background light.

The analysis above shows that when $V_B < V_{\mathrm{th}}$, the device has the bistability, and its I-I_m relation becomes the characteristic curve of bistability (namely, hysteresis curve); when $V_B > V_{\mathrm{th}}$, the device has only the single stable state, and its I-I_m relation becomes the characteristic curve of single stable state. Thus, for a given width of the sampling slit, bipolar switching voltage and intensity of the background light, the bistability of the device can always be achieved by changing the position of the sampling slit or the bias voltage.

IV. EXPERIMENTAL RESULTS

In order to describe the experimental results conveniently, the current A of the output detector is used to represent the sampling output optical intensity I, and the A corresponding to I_m is written as A_m, thus the character of the device can be expressed by the A-A_m curve. As a result, using the relation $D = I/I_m = A/A_m$, Eq. (3) can be rewritten as

$$D=(V-V_B)/K_A A_m, \tag{7}$$

where K_A is the feedback coefficient of A to V, and is determined by the characteristic curves of the amplifier.

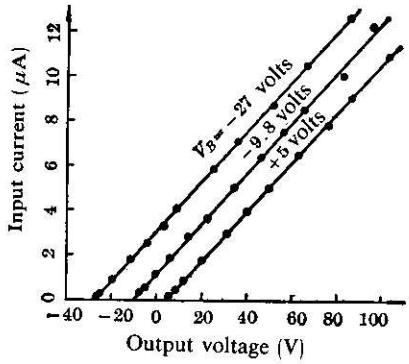

FIG. 3. Characteristic curves of the amplifier.

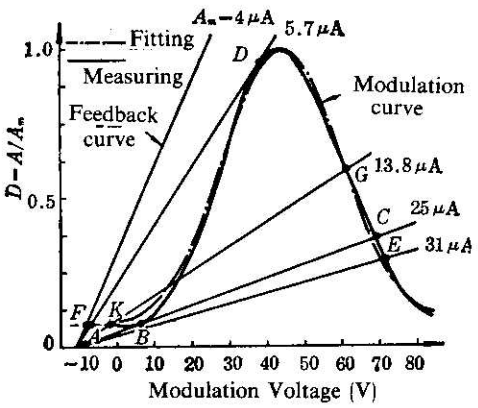

FIG. 4. The modulation and feedback characteristic curves at $V_B = -11.3$ V.

For $V_B = -27$, -9.8 and 5 V, the characteristic curves of the amplifier were measured by using a digital voltage meter. These curves are shown in Fig. 3, where the ordinate and the abscissa are the input current and output voltage of the amplifier, respectively, and the points represent the experimental values. From Fig. 3, it may be seen that the linearity of the amplifier is very good within the range of applied bias voltage, and K_A is 8.9 V/μA, and its error is about 5%.

When the slit width is between one fifth to one sixth of the output beam aperture, the modulation curve was measured by the recorder by continuously changing the modulation voltage. Least square fit by Eq. (2) is made after normalization. The fitting parameters are $D_s = 0.065$, $V_m = 44.5$ V, and $V_d = 22$ V. Substituting these parameters into Eq. (6), $V_{th} = 11.6$ V was obtained. The measured and fitted curves of the modulation are shown in Fig. 4 as the solid and dotted-dashed lines, respectively. The fitting results show that the Gaussian function model of the modulation curves basically agrees with the measured results when the slit width is smaller than the output beam aperture, and can be used to describe the properties of the bistability.

For $V_B = -11.3$ V, $K_A = 8.9$ V/μA is substituted into Eq. (7), a series of feedback curves were plotted using A_m as parameter (see Fig. 4). Using the intersection of the modulation curve and the feedback curves in Fig. 4, the hysteresis curve of A-A_m is calculated and is shown in Fig. 5. The tangential point D and the intersection point A in Fig. 4 correspond to the high and low output states of the leading edge of the hysteresis curve in Fig. 5, respectively, and the range of modulation voltage is V_D-$V_A \approx 46$ V; the intersection point C and the tangential point B correspond to the high and low output states of the lagging edge of hysteresis curve, and the range of modulation voltage is V_c-$V_B \approx 64$ V.

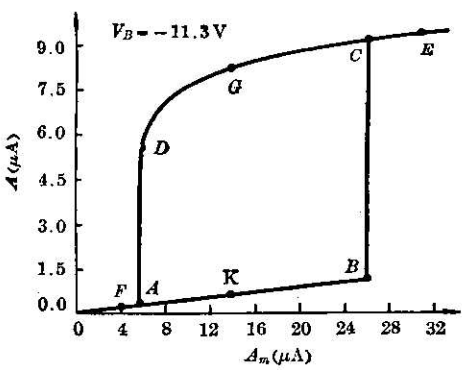

FIG. 5. The graphical hysteresis curve at $V_B = -11.3$ V.

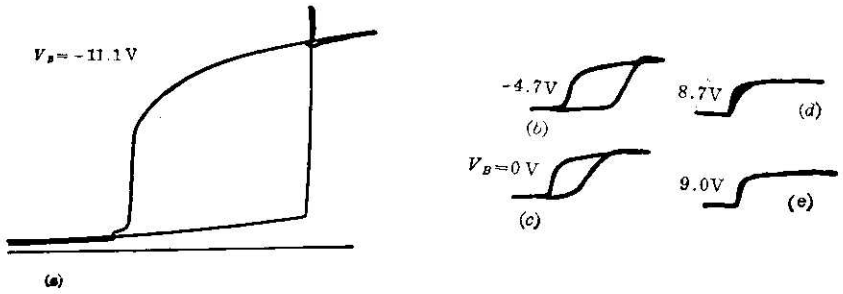

FIG. 6. The measured characteristics curves (hysteresis curves) of the device at $V_B = -11.1$, -4.7, 0, 8.7, and 9.0 V.

For comparison, by continuously changing the input light intensity by the optical attenuator at $V_B = -11.1$ V, the hysteresis curve of the bistability is plotted by the recorder, and is shown in Fig. 6(a), where V_D-$V_A = 46$ V, V_C-$V_B = 62$ V were measured using the digital voltmeter. It can be seen from Fig. 5 and 6(a) that the graphical and measured hysteresis curves not only are similar in shape, but the values of V_D-V_A and $V_{C\text{-}V_B}$ also in agree with each other basically.

Under different bias voltages ($V_B = -4.7$, 0,8.7, 9), the characteristic curves with different shapes are plotted by the recorder, and are shown in Fig. 6(b), (c), (d), and (e). Obviously, only when $V_B < 9$ V, the bistable states can be achieved.

To test the functions of the optical storage and the switching of the optical guided-wave beam deflector, the conversion between two stable output states were acheived using trigger of the positive and negative light pulses, and its oscillograph photo is shown in Fig. 7.

V. DISCUSSION

The experimental results show that the Gaussian function model of the modulation curve is suitable for the situations of the narrower sampling slits. Nevertheless, the slit width cannot be too narrow; otherwise, the higher input light intensity must be used to achieve the bistability. When the slit width is comparable to the output beam aperture, the modulation curve cannot be described by the Gaussian function. When the slit is too wide, there is no obvious inflection point on the modulation curve, hence the bistability cannot be easily achieved. Furthermore, the modulation curve is obviously broadened, the values of V_D-V_A and V_C-V_B become large, thus the switching energy is increased markedly.

There exists some difference between the threshold bias voltage (theoretical value; $V_{th} = 11.6$ V) obtained by the fitting of the modulation curve in Fig. 4 and the measured values of $V_{th} \approx 9$ V obtained by the characteristic curve in Fig. 6. There may be two reasons. First, the measured and fitted modulation curves were not completely consistent as shown in Fig. 4; it

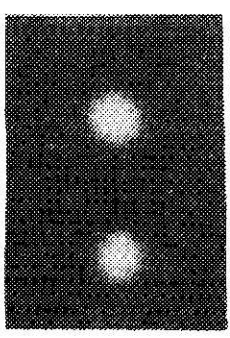

FIG. 7. The oscillograph photo for the conversion between two stable states.

shows that the Gaussian model of the modulation curve and the measured characteristics have some difference. Second, when the modulation curve in Fig. 4 and the characteristic curve in Fig. 6 were measured by the recorder, the former was measured at low speed and the latter was measured at fast speed, thus the mechanical inertia and response time of the recorder can also lead to experimental error.

The $LiNbO_3$ waveguide electro-optic prism used in this paper has higher switching voltage, thus the electric amplifier must be used to achieve the bistability. By using the waveguide electro-optic prism array[12] and improving the structure and size of the electrode, the bipolar switching voltage can be reduced to several volts so that the feedback circuit may be omitted. Such an optical guided-wave beam deflector can be used to construct the self-contained integrated optic bistable device.[2]

In summary, the bistabilities of the optical guided-wave beam deflector have been demonstrated experimentally and theoretically, providing scientific basis for developing the new integrated optic bistable device.

[1]P. W. Smith *et al.*, Appl. Phys. Lett., 1978, **33**, No. 1 (Jul), 24.
[2]P. W. Smith *et al.*, Appl. Phys. Lett., 1979, **34**, No. 1 (Jan), 62.
[3]E. Garmire *et al.*, Opt. Lett., 1978, **3**, No. 2 (Feb), 69.
[4]P. C. Cross *et al.*, IEEE J. Q. E., 1978, **QE-14**, No. 8 (Aug), 577.
[5]H. Ito *et al.*, Electron Lett., 1978, **15**, No. 24 (Nov), 791.
[6]A. Schnapper *et al.*, Opt. Commun., 1979, **29**, No. 3 (Jun), 364.
[7]H. Ito *et al.*, Electron. Lett., 1978, **15**, No. 10 (May), 283.
[8]W. Sohler; Appl. Phys. Lett., 1980, **36**, No. 5 (Mar), 351.
[9]H. F. Schlaak *et al.*; Opt. Commun., 1980, **32**, No. 1 (Jan), 72.
[10]I. P. Kaminow, L. W. Stulz; IEEE J. Q. E., 1975, **QE-11**, No. 8 (Aug), 633.
[11]Li Yushan; ⟨⟨Acta Optica Sinica⟩⟩, 1981, **1**, No. 1 (Jan), 93.
[12]C. S. Tsai *et al.*, Appl. Phys. Lett., 1975, **27**, No. 4 (Aug), 248.

Translation furnished by the authors
Edited by Tung Tsang